

New Metal Complexes Derived from Azo Linked Schiff-Base ligand: Synthesis, Spectral Investigation and Biological Evaluation

Mariam Basaim Hamza and Enaam Ismail Yousif*

Department of Chemistry, College of Education for Pure Science (Ibn Al-Haitham), University of Baghdad, Baghdad, Iraq



ARTICLE INFO

Received: 04 / 08 /2023
Accepted: 24 / 08 / 2023
Available online: 14/ 12/ 2023

DOI:10.37652/juaps.2023.142314.1108

Keywords:

Azo Linked Schiff-Base ligand;
Complexes; *p*-anisidine; Antimicrobial activity; Thermal properties.

Copyright©Authors, 2022, College of Sciences, University of Anbar. This is an open-access article under the CC BY 4.0 license (<http://creativecommons.org/licenses/by/4.0/>).



ABSTRACT

A new azo-Schiff base ligand derived from a *p*-anisidine molecule, as well as its monomeric metal complexes, were synthesized and studied. The titled ligand, (1-((E)-((4-methoxy phenyl) imino) methyl)-3-((E)-(4-nitrophenyl)diazenyl) naphthalen-2-ol) (HL), was synthesized by a 1:1 mole ratio reaction of *p*-anisidine and ((E)-2-hydroxy-3-((4-nitrophenyl)diazenyl). In a mole ratio of 1:1 (L:M), the interaction of HL with chosen metal ions, including Cr(III), Mn(II), Co(II), Ni(II), and Cu(II), resulted in the creation of monomeric coordination compounds. The synthesized compounds were analyzed using a variety of analytical and spectroscopic techniques. Elemental microanalysis, ¹H and ¹³C NMR, FT-IR, electronic and mass spectra, magnetic susceptibility, and conductance are among the techniques used. The synthesis of six and four-coordinate coordination molecules was confirmed by characterization data. Thermal stability (TGA) of HL and Co-complex is investigated. The antibacterial activity of the synthesized compounds was investigated against a variety of microorganisms (bacteria and fungus species). According to the data gathered, the ligand's antibacterial effectiveness improved after forming a complex..

INTRODUCTION

The azo compounds or dyes are characterized by the presence of the azo moiety (–N=N–) in their structure, conjugated with two, distinct or identical, mono- or polycyclic aromatic or hetero-aromatic systems[1]. The introduction of different functional groups to the backbone of a compound can significantly impact its electronic and structural flexibility, which can influence its range of potential applications [2]. Therefore, the design and synthesis of these compounds have become crucial areas of research for developing new materials with diverse applications [3]. An example of these species is the formation of Schiff bases that incorporate the azo moiety within their structure [4]. The introduction of the azo group may improve the properties of the compound for both biological and industrial applications [5].

The ability of Schiff bases to interact and form stable complexes with a wide range of metal ions makes them a crucial ligand in coordination chemistry [6,7]. Furthermore, the applications of Schiff bases are diverse and include their role in fields such as inorganic and analytical chemistry [8,9], as well as medicinal and pharmacological areas [10] and biological [11] Schiff bases with azo moieties have a wide range of applications beyond their use in biological systems. They can also be utilised as pigments or dyes [12-14], catalysts [15], intermediate agents, corrosion inhibitors [16], and polymer stabilizers [17]. Schiff bases have been utilized as a membrane in the ion-selective electrode approach for sensing ions [18]. The title azo-Schiff base ligand was created in two steps: first, the azo species (E)-2-hydroxy-3-((4-nitrophenyl)diazenyl)-1 naphthaldehyde, (L), was formed, followed by a reaction with *p*-anisidine to produce the title ligand (HL). The ligand was subsequently reacted in a mole ratio of 1:1 (L:M) with Cr(III), Mn(II), Co(II), Ni(II), and

*Corresponding author at: Department of Chemistry, College of Education for Pure Science (Ibn Al-Haitham), University of Baghdad, Baghdad, Iraq;
ORCID:<https://orcid.org/0000-0001-9529-8740> ; Tel:+9640000000000000
E-mail address: anaam.i.y@ihcoedu.uobaghdad.edu.iq

Cu(II)ions, resulting in the formation of monomeric paramagnetic complexes. The antibacterial and antifungal properties of the synthesised compounds were examined. This was aimed to explore the biological activity of compounds and to observe the impact of the metal ion and the coordination sphere of the compound on the biological activity of the ligand upon complexation.

Experimental

Materials and Methods: The NMR spectra (^1H and ^{13}C -NMR) for the ligand were recorded in dimethyl sulfoxide using a Bruker 400 MHz instrument (400 MHz for ^1H and 100 MHz for ^{13}C). FT-IR spectra were recorded as potassium bromide discs in the range 4000-400 cm^{-1} using FTIR-600 Fourier Transform Infrared Spectroscopy. Electrospray (+) mass spectroscopy was performed on a SciexEsi mass analysis. An electrothermal Stuart apparatus, model SMP40, was used to determine melting points. The electronic spectra were acquired in the region 1000-200nm using a quartz cell of (1.0) cm length with a concentration of 10^{-3}mol L^{-1} of samples in DMSO at 25 °C using an electronic spectra spectrophotometer type Shimadzu UV-160. A Eutech Instruments Cyber scan with 510 digital conductivity meter was used to assess the complexes' molar conductivity at 25 °C for 10^{-3} – 10^{-5} M solutions of the compounds in DMSO. A Heraeus instrument (Vario EL) and a Shimadzu (A A-7000) atomic absorption spectrophotometer were used to determine the metal percentage and elemental analysis (C, H, and N), respectively. The amount of chloride in the complexes was measured using a potentiometric titration method on the 686–Titro Processor-665 Dosim A-Metrohm / Switzerland. Thermal gravimetric analysis (TGA) of the substances was performed using a STA PT-1000 Linseis Company / Germany analyzer. Magnetic moments at 303 K were quantified using a magnetic moments balance on Johnson Matthey.

Synthesis

The formation of the azo Schiff ligand was achieved in two steps and as follows;

Preparation of (L)

The following documented procedure [19,20] was used to prepare (L): 20 ml of an ethanol-water (10-10) solution were added to a 250 ml round-bottomed flask that had previously been charged with sodium nitrite (0.69 g, 10 mm) and 1-amino-4-nitrobenzene (1.38 g, 10.01 mm). The mixture was cooled to 0-5°C in an icy bath and then a solution of 3ml of hydrochloric acid (36%) with 10ml of water was added dropwise with stirring over a period of 1h. The obtained diazonium salt solution was then coupled with the cooled mixture of NaOH (0.4g, 10mm) and 2-hydroxy-1-naphthaldehyde (1.72g, 10.01mm). The reaction mixture was allowed to stir for 2h. The resulting precipitate was filtered at pH 4 and then washed thoroughly with cold water and left to dry at pH 6-7. The precipitate that was orange-red was filtered out then rinsed with 5ml of cold ethanol before air-drying, Yield: 2.09g (65%), m.p. 254-256°C.

Preparation of the ligand: The preparation of HL was accomplished using a general procedure reported in [10] as well as the following: *p*-anisidine (0.119g, 0.933mmol) in 10ml ethanol with three drops glacial acetic acid was added with stirring to a mixture of (L) (0.3g, 0.933mmol) in 20ml of a mixture of ethanol–benzene (1:1). The reaction mixture was heated to 70-80 °C for 6h. After filtering the solution while it was still hot, RT was allowed to allow it to slowly evaporate. After being crushed out of the solution, the orange powder was gathered, dried in the air, and then recrystallized from ethanol. 0.353g (88.60%), m.p. = 120–122°C, yield.

Preparation of complexes: An analogous procedure to that reported for the Cr(III)-complex was adopted to prepare complexes as follows; To a mixture of HL (0.2g, 0.469mmol) in 10ml of EtOH was added an ethanolic solution of KOH (0.03g, 0.469mmol) in 10ml EtOH. The mixture was stirred and a solution of $\text{CrCl}_3 \cdot 6\text{H}_2\text{O}$ (0.12g, 0.469mmol) dissolved in ethanol (5ml) was added dropwise. The stirred reaction mixture was heated at reflux for 3h and the solid that formed was filtered off, washed with cold ethanol and dried in air. Yield: 0.15g (56.47%), m.p. >300°C. Scheme (1). Table 1 lists the complexes' yields, colors, amounts of metal salts, and melting points.

Microbiological Evaluation: The Kirby-Bauer technique was used to test bacteria and fungal sensitivity to the produced compounds. The organisms were

combined with a (85 percent Sodium Chloride) solution until a suspension was formed (1/2 M.C.f). This suspension was applied to the surface using a Petri plate filled with Mueller Hinton agar. All of the holes were made at the same distance and with the same degree of concentration. The preferred concentration (100 L) of the test sample (1 mg/mL) in dimethylsulfoxide was used in the wells. The zone of inhibition was measured and compared to the standard values after 24 hours of incubation at 37 °C. Separate research on the effect of dimethylsulfoxide solutions on microbiological testing revealed that they had no effect

Table 1: Yields, colours, metal salts quantities and melting points of compounds.

Complexes	Weight of metal salt(g)	Weight of complex(g)	Colour	m.p.°C	Yield (%)
[Cr(L)Cl ₂ .H ₂ O]	0.12	0.15	Brown	>300*	56.47
[Mn(L)Cl(H ₂ O) ₂]	0.09	0.17	Reddish-brown	285-287	65.68
[Co(L)Cl].H ₂ O	0.11	0.21	Yellow	296-298	80.98
[Ni(L)Cl(H ₂ O) ₂]	0.11	0.16	Dark Green	>300*	61.40
[Cu(L)Cl(H ₂ O) ₂]	0.08	0.18	Yellowish-brown	250-252	68.47

*= Decomposed.

RESULTS AND DISCUSSION

Making the azo Schiff base ligand (1-(((4-methoxyphenyl)imino)methyl)-3-((E)-(4-nitrophenyl) diazenyl) naphthalen-2-ol) (HL) was accomplished from the reaction of (L) with (*p*-anisidine) in a mole ratio of 1:1 in EtOH medium (Fig. 1). The potentially monobasic multidentate azo Schiff ligand was reacted with Cr(III), Mn(II), Co(II), Ni(II) and Cu(II) metal chlorides in a 1:1

(L:M) mole ratio yielding six and four-coordinate monomeric paramagnetic coordination compounds of the general formula [Cr(L)Cl₂.H₂O], [M(L)Cl.(H₂O)₂] where M= where M= Mn(II), Ni(II), Cu(II) and [Co(L)Cl].H₂O Scheme 1. The isolated monomeric compounds are solids that are stable in the air, that dissolving in dimethylsulfoxide and dimethylformamide. The obtained microanalysis data including the metal and chloride contents of compounds are in good agreement with the calculated values, Table 2. The molar conductance of the complexes in DMSO solutions indicated that the complexes are nonelectrolytes.

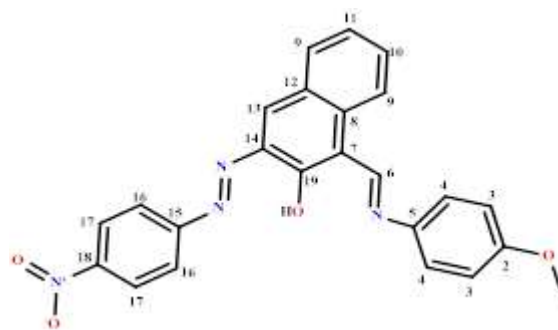
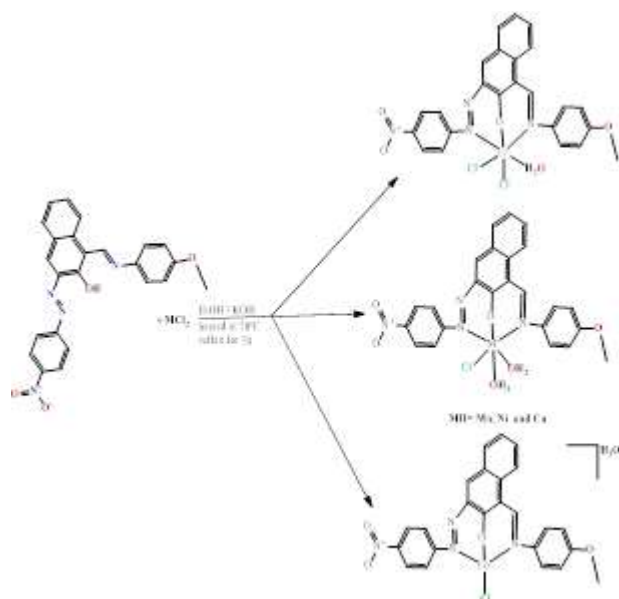


Figure1: Chemical structure of HL.

Table 2: Physical Properties and Microanalysis of the HL and its complexes clusters

Complex	Molecular formula	M.Wt	Micro analysis found, (calculated)%				
			C	H	N	M	Cl
[Cr(L)Cl ₂ .H ₂ O]	C ₂₄ H ₁₉ Cl ₂ CrN ₄ O ₅	566.34	(50.90) 50.35	(3.38) 3.14	(9.89) 9.22	(9.18) 9.02	(12.52) 12.00
[Mn(L)Cl(H ₂ O) ₂]	C ₂₄ H ₂₁ ClMnN ₄ O ₆	551.84	(52.24) 52.02	(3.84) 3.21	(10.15) 10.00	(9.96) 9.41	(6.42) 6.13
[Co(L)Cl].H ₂ O	C ₂₄ H ₁₉ ClCoN ₄ O ₅	552.86	(54.31) 54.11	(4.01) 3.95	(10.13) 10.00	(10.66) 10.41	(6.41) 6.19
[Ni(L)Cl(H ₂ O) ₂]	C ₂₄ H ₂₁ ClNiN ₄ O ₆	555.60	(51.88) 51.15	(3.81) 3.39	(10.08) 9.91	(10.56) 10.27	(6.38) 6.18

$[\text{Cu(L)Cl}(\text{H}_2\text{O})_2]$	$\text{C}_{24}\text{H}_{21}\text{ClN}_3\text{O}_6$	560.45	(51.43)	(3.78)	(10.00)	(11.34)	(6.33)
	uN_4O_6		51.14	3.54	9.86	11.12	6.00



Scheme 1: General synthesis route of HL complexes.

FT-IR and NMRdata:

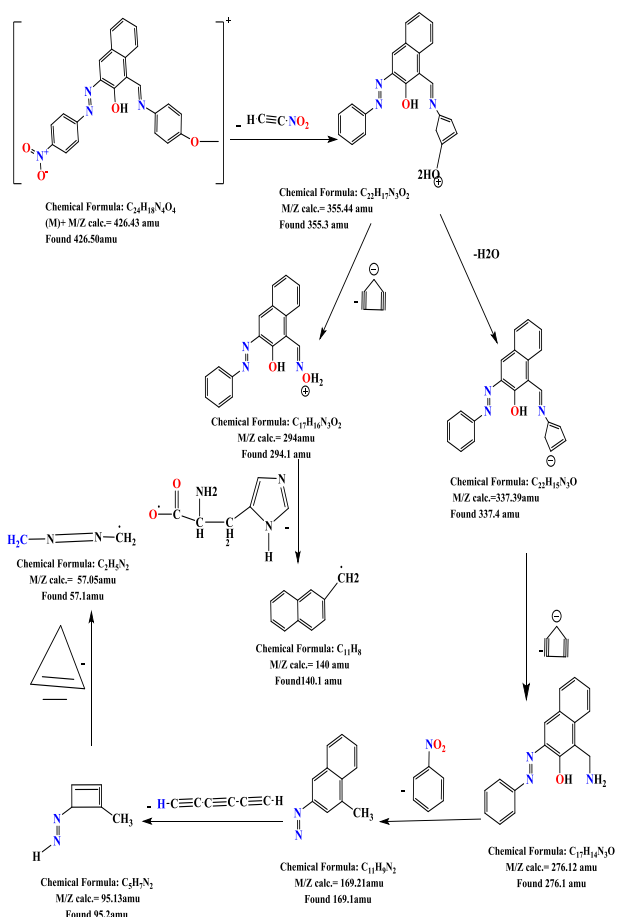
The main infrared bands of complexes along with their assignments are listed in Table 3. There was a peak in the HL spectrum at 3421cm^{-1} due to the $\nu(\text{OH})$ of the phenolic group [22]. The band observed at 1635cm^{-1} is due to $\nu(\text{C}=\text{N})$ of the imine group. The spectra of Cr(III) , Mn(II) , Co(II) , Ni(II) and Cu(II) revealed a distinctive range at $1623\text{--}1618\text{cm}^{-1}$ that correlated to $\nu(\text{C}=\text{N})$ imine. The appearance of this band upon complexation accounts for the coordination of the metal ion with the nitrogen atom of the azomethine group $\nu(\text{C}=\text{N})$ imine [23]. The band in HL that was associated to the $\nu(\text{N}=\text{N})$ azo group and was detected at 1462cm^{-1} was displaced to emerge at 1454 , 1458 , 1456 , 1485 , and 1454cm^{-1} in Cr(III) , Mn(II) , Co(II) , Ni(II) , and Cu(II) , respectively. This may be connected to how the complexation involved the nitrogen atom. Furthermore, additional bands between $(600\text{--}400)\text{cm}^{-1}$ that were not visible in the HL spectrum were seen in the metal complexes' spectra. Bands associated with $\nu(\text{M-O})$ were discovered between and $(586\text{--}540)\text{cm}^{-1}$ [25]. The FT-IR spectra detected peaks correlated to $\nu(\text{Cr-N})$, $\nu(\text{Mn-N})$, $\nu(\text{Co-N})$, $\nu(\text{Ni-N})$ and $\nu(\text{Cu-N})$ in the range $(468\text{--}416)\text{cm}^{-1}$ [26]. The bands identified in the FT-IR spectra are associated with $\nu(\text{Cr-Cl})$, $\nu(\text{Mn-Cl})$, $\nu(\text{Co-Cl})$, $\nu(\text{Ni-Cl})$, and $\nu(\text{Cu-Cl})$ and are located at 223 ; 291 , 264 , 241 , 298 , and 217cm^{-1} , respectively [27]. Finally, peaks were detected at 3450 , 3398 , 3431 , 3512 and 3438cm^{-1} in the spectra of Cr(III) , Mn(II) , Co(II) , Ni(II) and Cu(II) , respectively. These were correlated to aqua water molecules. In complexes Cr(III) , Mn(II) , Co(II) , Ni(II) and Cu(II) , bands that were detected at 750 , 750 , 748 and 752cm^{-1} are related to $\nu(\text{Cr-O})$, $\nu(\text{Mn-O})$, $\nu(\text{Ni-O})$ and $\nu(\text{Cu-O})$ coordinated water [27]. The ^1H NMR spectra of HL^1 is illustrated in Fig (2). The spectrum indicated two sets of signals in the aliphatic and aromatic regions. The aromatic region showed several chemical shifts between $8.970\text{--}7.602\text{ppm}$. The chemical shift at $8.970\text{--}8.949\text{ppm}$ that is equivalent to three protons and appears as a singlet is related to $(\text{C}_{13})\text{-H}$ (3H , t, $J = 8.4\text{Hz}$). The chemical shift at $8.528\text{--}8.507\text{ppm}$ that is equivalent to two protons and appears as a singlet is related to $(\text{C}_{17,17'})\text{-H}$ (2H , d, $J = 8.4\text{Hz}$). The chemical shift at $8.131\text{--}8.108\text{ppm}$ that is equivalent to three protons and appears as a doublet is related to $(\text{C}_{9,9'})\text{-H}$ (3H , t, $J = 9.2\text{Hz}$). The chemical shift at $7.992\text{--}7.924\text{ppm}$ that is equivalent to two protons and appears as a doublet is related to $(\text{C}_{16,16'})\text{-H}$ (2H , d). The chemical shift at $7.886\text{--}7.824\text{ppm}$ that is equivalent to two protons and appears as a doublet is related to $(\text{C}_{4,4'})\text{-H}$ (2H , d, $J = 7.6\text{Hz}$). The three sets of the triplet peak at $7.695\text{--}7.602\text{ppm}$ that is equal to three protons and is credited to $(\text{C}_{10})\text{-H}$ (3H , t), the three sets of the triplet peak at $7.385\text{--}7.311\text{ppm}$ that is equal to three protons and is credited to $(\text{C}_{11})\text{-H}$ (3H , t) and the chemical shift at $7.085\text{--}7.026\text{ppm}$ that is equivalent to two protons and appears as a singlet is related to $(\text{C}_3)\text{-H}$ (2H , d). A signal at $10.809\text{--}10.360\text{ppm}$ that belongs to OH and is equivalent to one proton (1H , OH, s). A signal at 9.653ppm that belongs to $(\text{C}_6)\text{-H}$ proton of $\text{CH}=\text{N}$ and is equivalent to one proton (1H , $\text{CH}=\text{N}$, s). The singlet peak at $1.071\text{--}1.038\text{ppm}$ that is equal to three protons is allocated to the CH_3 group ($\text{C}_1\text{-H}$) (3H , s, $\text{O}(\text{Me})$). The DMSO-d_6 solution produced peaks in the spectrum, as well as traces of water molecules at 2.508 and $3.381\text{--}3.433\text{ppm}$, consecutively. The ^{13}C -NMR spectrum of HL^1 is illustrated in Fig(3). The resonances at $\delta = 168.39$, 164.58 , $159.21\text{--}159.10$, 155.70 , 138.74 , 137.65 and 136.32ppm were assigned to (C_2) , (C_{16}) , (C_6) , (C_{19}) , (C_{20}) , (C_5) and (C_{15}) , respectively. Signals related to (C_8) , (C_{14}) , (C_{13}) , (C_{12}) , (C_{10}) , $(\text{C}_{18,18'})$, (C_{11}) and $(\text{C}_{4,4'})$

$\text{Cl})$, $\nu(\text{Mn-Cl})$, $\nu(\text{Co-Cl})$, $\nu(\text{Ni-Cl})$, and $\nu(\text{Cu-Cl})$ and are located at 223 ; 291 , 264 , 241 , 298 , and 217cm^{-1} , respectively [27]. Finally, peaks were detected at 3450 , 3398 , 3431 , 3512 and 3438cm^{-1} in the spectra of Cr(III) , Mn(II) , Co(II) , Ni(II) and Cu(II) , respectively. These were correlated to aqua water molecules. In complexes Cr(III) , Mn(II) , Co(II) , Ni(II) and Cu(II) , bands that were detected at 750 , 750 , 748 and 752cm^{-1} are related to $\nu(\text{Cr-O})$, $\nu(\text{Mn-O})$, $\nu(\text{Ni-O})$ and $\nu(\text{Cu-O})$ coordinated water [27]. The ^1H NMR spectra of HL^1 is illustrated in Fig (2). The spectrum indicated two sets of signals in the aliphatic and aromatic regions. The aromatic region showed several chemical shifts between $8.970\text{--}7.602\text{ppm}$. The chemical shift at $8.970\text{--}8.949\text{ppm}$ that is equivalent to three protons and appears as a singlet is related to $(\text{C}_{13})\text{-H}$ (3H , t, $J = 8.4\text{Hz}$). The chemical shift at $8.528\text{--}8.507\text{ppm}$ that is equivalent to two protons and appears as a singlet is related to $(\text{C}_{17,17'})\text{-H}$ (2H , d, $J = 8.4\text{Hz}$). The chemical shift at $8.131\text{--}8.108\text{ppm}$ that is equivalent to three protons and appears as a doublet is related to $(\text{C}_{9,9'})\text{-H}$ (3H , t, $J = 9.2\text{Hz}$). The chemical shift at $7.992\text{--}7.924\text{ppm}$ that is equivalent to two protons and appears as a doublet is related to $(\text{C}_{16,16'})\text{-H}$ (2H , d). The chemical shift at $7.886\text{--}7.824\text{ppm}$ that is equivalent to two protons and appears as a doublet is related to $(\text{C}_{4,4'})\text{-H}$ (2H , d, $J = 7.6\text{Hz}$). The three sets of the triplet peak at $7.695\text{--}7.602\text{ppm}$ that is equal to three protons and is credited to $(\text{C}_{10})\text{-H}$ (3H , t), the three sets of the triplet peak at $7.385\text{--}7.311\text{ppm}$ that is equal to three protons and is credited to $(\text{C}_{11})\text{-H}$ (3H , t) and the chemical shift at $7.085\text{--}7.026\text{ppm}$ that is equivalent to two protons and appears as a singlet is related to $(\text{C}_3)\text{-H}$ (2H , d). A signal at $10.809\text{--}10.360\text{ppm}$ that belongs to OH and is equivalent to one proton (1H , OH, s). A signal at 9.653ppm that belongs to $(\text{C}_6)\text{-H}$ proton of $\text{CH}=\text{N}$ and is equivalent to one proton (1H , $\text{CH}=\text{N}$, s). The singlet peak at $1.071\text{--}1.038\text{ppm}$ that is equal to three protons is allocated to the CH_3 group ($\text{C}_1\text{-H}$) (3H , s, $\text{O}(\text{Me})$). The DMSO-d_6 solution produced peaks in the spectrum, as well as traces of water molecules at 2.508 and $3.381\text{--}3.433\text{ppm}$, consecutively. The ^{13}C -NMR spectrum of HL^1 is illustrated in Fig(3). The resonances at $\delta = 168.39$, 164.58 , $159.21\text{--}159.10$, 155.70 , 138.74 , 137.65 and 136.32ppm were assigned to (C_2) , (C_{16}) , (C_6) , (C_{19}) , (C_{20}) , (C_5) and (C_{15}) , respectively. Signals related to (C_8) , (C_{14}) , (C_{13}) , (C_{12}) , (C_{10}) , $(\text{C}_{18,18'})$, (C_{11}) and $(\text{C}_{4,4'})$

were detected at 133.46,132.10,129.74-129.26,128.75-128.00,127.34,126.05, 124.98-124.15 and 122.84-122.77ppm, respectively. The chemical shifts that appeared at 121.38-121.23,117.63,108.63,56.49-55.90and19.03ppm are assigned to ($C_{17,17^-}$), (C_9), ($C_{3,3^-}$), (C_7) and (C_1),respectively. The spectrum revealed peak at 39.31-40.56ppm which is associated with the solvent (DMSO- d_6).

Mass spectrum:

The electrospray (+) mass spectrum of HL, Fig4, displays the parent ion peak at $M/Z=426.50$ amu. This peak is related to $(M)^+$. The assignment of the fragmentation ions and their relative abundance is shown in Scheme (2).



Scheme 1: The relative quantity and fragmentation distribution of HL pieces

Electronic spectra (UV-Vis) and magnetic susceptibility:

Data on the magnetic moments and electronic spectra are compiled in Table 4. The compounds'

electronic spectra showed a number of peaks near 271-264nm, which can be attributed to $\pi \rightarrow \pi^*$ and $n \rightarrow \pi^*$, respectively. The additional peaks observed near 491-455 nm were assigned as charge transfer (C.T) [28,29]. The electronic spectrum of the Cr(III)-complex exhibits bands at 681 and 987 nm due to $^4A_{2g} \rightarrow ^4T_{2g}$ and $^4A_{2g} \rightarrow ^4T_{1g(F)}$, revealing a distorted octahedral structure. This assignment is consistent with the Cr-complex magnetic moment value of 3.75. A deformed octahedral structure around the Mn center is confirmed by a band in the d-d region at 891 nm associated to $6A_{1g} \rightarrow 4E_g(D)$ in the electronic spectra of $[Mn(L)Cl(H_2O)_2]$. The 5.75 Mn(II)-complex magnetic moment value is consistent with this assignment. The d-d area at 755 nm in the $[Co(L)Cl] \cdot H_2O$ disclosed band is caused by $4T_1(F) \rightarrow 4A_2(F)$, which indicates a four-coordinated complex with a tetrahedral shape surrounding the Co(II) center. The magnetic moment value $\mu_{eff} = 4.28$ BM for the complex is consistent with the tetrahedral configuration around the Co atom [29,30]. An octahedral structure surrounding the metal center was revealed by a peak in the Ni(II)-complex at 890 nm, which was ascribed to $3A_{2g} \rightarrow 3T_{1g(F)}$. The octahedral shape agrees with the magnetic moment value $\mu_{eff} = 3.73$ BM of the Ni(II)-complex. The $[Cu(L)Cl(H_2O)_2]$ spectrum revealed a peak at 741 nm, which was attributed to $^2T_{2g} \rightarrow ^2B_{2g}$, indicating a distorted octahedral arrangement about the metal centre [29,30]. The copper complex's $\mu_{eff} = 1.82$ BM magnetic moment value is consistent with the distorted octahedral shape.

Table 3: The FT-IR spectral data of compounds (cm^{-1})

Compounds	$\nu(C=N)$	$\nu(C=C)$	$N=N=N$	$\nu N-O$ $\nu N-O$	$\nu C-O$ $\nu C-N$	$\nu(M-O)$	$\nu(M-OH)$	$\nu M-N$	$\nu M-Cl$
HL	1635	1604, 1573	1462	1512, 1354	1300 1257	-	-	-	
$[Cr(L)Cl_2 \cdot H_2O]$	1623	1604, 1552	1454	1512, 1357	1334, 1255	540	3450 750	468	291, 223

[Cu(L) Cl(H ₂ O) ₂]	[Ni(L) Cl(H ₂ O) ₂]	[Co(L) Cl]. H ₂ O	[Mn(L) Cl(H ₂ O) ₂]
1622	1623	1618	1622
1593,	1600,	1591,	1581,
1556	1548	1541	1548
1454	1485	1456	1458
1510,	1512,	1506,	1506,
1398	1357	1367	1394
1336,	1328,	1344,	1334,
1228	1255	1249	1228
557	540	580	586
3438	3512	3431	3398
752	748		750
468	460	451	416
217	298	241	264

Table 4 shows the electronic spectra of HL complexes in DMSO solutions.

Complex	λ (nm)	Molar extinction coefficient ϵ_{\max} (dm ³ mol ⁻¹ cm ⁻¹)	Assignment	μ_{eff}	Suggested geometry
[Co(L)Cl ₂ H ₂ O]	267 316 489 681 987	556 476 483 42 52	Ligand field Ligand field Charge transfer $^4A_{2g} \rightarrow ^2T_{1g}$ $^4A_{2g} \rightarrow ^2T_{2g}^{(F)}$	3.75	Distorted octahedral
[Mn(L)Cl ₂ (H ₂ O) ₂]	267 324 479 891	986 739 1237 23	Ligand field Ligand field Charge transfer $^6A_{1g} \rightarrow ^4E_g^{(D)}$	5.75	Distorted octahedral
[Co(L)Cl ₂ H ₂ O]	267 328 486 755	958 820 2190 32	Ligand field Ligand field Charge transfer $^4T_{1g}^{(F)} \rightarrow ^4A_{2g}^{(F)}$	4.28	Tetrahedral
[Ni(L)Cl ₂ (H ₂ O) ₂]	271 327 491 890	317 250 582 11	Ligand field Ligand field Charge transfer $^3A_{2g} \rightarrow ^3T_{1g}^{(F)}$	3.73	Distorted octahedral
[Cu(L)Cl ₂ (H ₂ O) ₂]	264 346 455 741	689 348 193 9	Ligand field Ligand field Charge transfer $^2T_{2g} \rightarrow ^2B_{2g}$	1.82	Distorted octahedral

Thermal analysis: An argon atmosphere was used for the solid ligand (HL) thermal breakdown

analysis. We measured the weight loss from room temperature to 550°C. According to the TGA data, the ligand breaks down in four stages (Fig. 5). The TGA curve at 95-169°C, which shows the weight loss at the first peak, may be related to the loss of (H₂O) segments (obs. = 0.711mg, 4.292%; calc. = 0.711mg mg, 4.221%). The loss of the (2H₂ +NH₃) segment may be shown by the second step measured at 192-235°C (obs.= 0.818 mg, 4.938%; calc.0.817 mg, 4.924 %).(CO+H₂O) segment is linked to the third phase, which occurs between 249 and 303°C (obs. = 1.810mg, 10.927%; calc. = 1.80mg, 10.78%). The (C₆H₆+HCN+CO) segment may have been lost, as shown by the fourth step reported at 309–446°C (obs.=5.152mg, 31.102%;

calc.=31.189mg,5.166%). The remaining components of the(C₁₆HN₂) calc.=208.43mg,48.777. The first peak may be related to the melting point of the ligand. The thermogram of the [Co(L)Cl].H₂O complex proceeds in two steps, Fig 6. The initial peak measured at 64-107°C may be due to loss of molecules from the (H₂O) segment; (obs.=0.250mg, 3.091%; calc.= 0.263mg, 3.255%). The second step happened at 408-529°C showed the loss of (CO+2N₂+3H₂) fragment;(obs.= 1.296mg, 16.022%; calc.=1.291mg ,16.278%). The remaining components of the (CoO₂+C₂₂H₁₁+Cl+CO) obs.=444.86mg, 80.465.

Biological activity: The antibacterial evaluation of the synthesized ligand HL and its metal complexes was carried out against four types of bacteria: *Staphylococcus aureus*, *Bacillus subtilis*, *Escherichia coli*, and *Pseudomonas aeruginosa*. The role of the DMSO solvent against the tested bacteria was excluded throughout separate investigations [31]. Further, the effect of the title compounds against the tested bacteria was compared with the commercial drug Gentamicin. Table 5 shows the inhibition zone results of the title compounds against the development of several bacterial strains. The recorded results indicated that the complexes were more active, Fig7. The experimental results concluded the following aspects:

1. Each compound demonstrated effectiveness against both positive and negative microorganisms.

- Based on the collected information, Co(II) - complex show greater microbiological activity against the bacteria tested.
- The metal complexes of HL showed moderate antibacterial activity, compared with Gentamicin.

Candida albicans was used as the test organism for the antifungal effectiveness of the HL ligand and its metal complexes. Separately, the function of DMSO in the biological screening was determined using DMSO-only solutions, which exhibited no activity towards fungal species. [32-38]. The commercial drug against fungus,

Metronidazole, has been used as a reference in this study. The results of the anti-fungal activity testing against the chemicals are displayed in Table 6. The findings include the following ones, Fig 7. The tested compounds showed excellent results against *Candida albicans*

The coordination compounds showed enhancement in the anti-fungal activity, compared with the free ligand. This may relate to the chelation effect.

- The Cr(III) and Co(II)-complexes indicated the highest inhibition activity against *Candida albicans*.
- The coordination compounds indicated excellent activity, compared with Metronidazole.

Table (5): The antibacterial activity inhibition zones (mm) for ligand and its complexes.

Compounds	<i>Escherichia coli</i> (G-)	<i>Pseudomonas aeruginosa</i> (G-)	<i>Staphylococcus aureus</i> (G+)	<i>Bacillus subtilis</i> (G+)
DMSO	-	-	-	-
Gentamicin	15	16	14	13
HL	7	7	8	7
[Cr(L)Cl ₂ .H ₂ O]	8	10	9	10
[Mn(L)Cl(H ₂ O) ₂]	10	9	12	9
[Co(L)Cl].H ₂ O	12	10	12	10
[Ni(L)Cl(H ₂ O) ₂]	8	7	10	7
[Cu(L)Cl(H ₂ O) ₂]	7	8	8	8

Table 6. shows the antifungal inhibition zones (mm) for HL and its complexes.

Compounds	<i>Candida albicans</i>
DMSO	-
Metronidazole	12
HL	7
[Cr(L)Cl ₂ .H ₂ O]	10
[Mn(L)Cl(H ₂ O) ₂]	9
[Co(L)Cl].H ₂ O	13
[Ni(L)Cl(H ₂ O) ₂]	9
[Cu(L)Cl(H ₂ O) ₂]	9



Bacillus subtilis



Staphylococcus aureus.



Pseudomonas aeruginosa



Escherichia coli



Candida albicans

Fig (7): The biological evaluation of HL and its complexes

Conclusions:

A new azo-Schiff base and its paramagnetic coordination compounds with Cr (III), Mn(II), Co(II), Ni(II) and Cu(II) are reported. The ligand (1-(((4-methoxyphenyl)imino)methyl)-3-((E)-(4-nitrophenyl) diazenyl) naphthalen-2-ol) (HL) was synthesized from the condensation of the azo aldehyde compound (L) with (*p*-anisidine) in a mole ratio of 1:1. By reacting the ligand at a mole ratio of 1:1 (L:M) with Cr (III), Mn(II), Co(II), Ni(II), and Cu(II) ions, monomeric complexes were isolated. Using a variety of physicochemical techniques, the compounds' entity, bonding mechanism, and general structure were all obtained. Furthermore, it was established how thermally stable the complexes and ligand were. Six and four-coordinate complexes were proposed in light of these results. The biological evaluation of the ligand and its coordination compounds against bacterial strains and fungi species revealed that the complexes became more active in comparison to the free ligand.

References:

- [1].Giovanni, D. A. R., Giuseppe, B., and Andrea, F.,2014. Quantitative Determination of 26 Aromatic Amines Derived from Banned Azo Dyes in Textiles Through the Use of LC, Tandem MS, and Identification of Some Structural Isomers.
- [2]. Hakimi, M., Kukovec, B. M., & Minoura, M. (2012). 2D sd Mixed-Metal Coordination Polymer Containing Potassium, Chromium (III) and Dipicolinate Ions: Preparation and Crystal Structure. *Journal of chemical crystallography*, 42(3), 290-294.
- [3].Hasan A. H, Enaam I.Y and Ahmed K. H.,Co^{II}, Ni^{II} and Cd^{II} complexes derived from mixed Azo-linked schiff-base ligands: Formation, characterisation, thermal analysis and biological study., (2020) *Journal of Plant Archives*.,V.20 (1). pp. 2405-2411.
- [4].E. I. Yousif.,Synthesis and Characterization of Novel Tetradentate ligand Type N4 and its Complexes With CoII,NiII,andPdII., IBN AL- HAITHAM J. FO R PURE & APPL. SC I., 22, 4, 1-13.
- [5]. Enaam I. Yousif and Hasan A. Hasan.,Formation of New Macrocyclic Complexes with bis(Dithiocarbamate) Ligand; Preparation, Structural Characterisation and Bacterial Activity., 2017.,IBN AL- HAITHAM J. FO R PURE & APPL. SC I 29 (3), 146-166.
- [6].Ahmed Ibrahim Ahmed, Enaam I.Y.,(New Metal Complexes with Azo ligand; Synthesis, Spectral Characterisation and Biological Evaluation),. 2550 M H S Vol. 16, No. 07, 2022
- [7].Enaam.I.Yousif and Hasan A. Hasan.,New Bis(dithiocarbamate) Ligand for Complex Formation; Synthesis, Spectral Analysis and Bacterial Activity.,2017., IBN AL- HAITHAM J. FO R PURE & APPL. SC I.,30,1, 73-87.
- [8]. Uddin, M. N., Siddique, Z. A., Mase, N., Uzzaman, M., &Shumi, W. (2019). Oxotitanium (IV) complexes of some bis-unsymmetric Schiff bases: Synthesis, structural elucidation and biomedical applications. *Applied Organometallic Chemistry*, 33(6), e4876.
- [9]. Ghosh, P., Dey, S. K., Ara, M. H., Karim, K., & Islam, A. B. M. (2019). A review on synthesis and versatile applications of some selected Schiff bases with their transition metal complexes. *Egyptian Journal of Chemistry*, 62(Special Issue (Part 2) Innovation in Chemistry), 523-547.
- [10]. Abdel-Shakour, M., El-Said, W. A., Abdellah, I. M., Su, R., & El-Shafei, A. (2019). Low-cost Schiff bases chromophores as efficient co-sensitizers for MH-13 in dye-sensitized solar cells. *Journal of Materials Science: Materials in Electronics*, 30(5), 5081-5091.
- [11]. Karrouchi, K., Brandán, S. A., Hassan, M., Bougrin, K., Radi, S., Ferbinteanu, M., & Garcia, Y. (2021). Synthesis, X-ray, spectroscopy, molecular docking and DFT calculations of (E)-N'-(2, 4-dichlorobenzylidene)-5-phenyl-1H-pyrazole-3-carbohydrazide. *Journal of Molecular Structure*, 1228, 129714.
- [12]. Nourifard, F., &Payehghadr, M. (2016). Conductometric studies and application of new Schiff base ligand as carbon paste electrode modifier for mercury and cadmium determination. *International Journal of Environmental Analytical Chemistry*, 96(6), 552-567.
- [13]. Singh, L. P., &Bhatnagar, J. M. (2004). Copper (II) selective electrochemical sensor based on Schiff Base complexes. *Talanta*, 64(2), 313-319.

- [14]. Al Zoubi, W., Al-Hamdani, A. A. S., &Kaseem, M. (2016). Synthesis and antioxidant activities of Schiff bases and their complexes: a review. *Applied Organometallic Chemistry*, 30(10), 810-817.
- [15]. Karman, M., &Romanowski, G. (2020). Cis-dioxidomolybdenum (VI) complexes with chiral tetradentate Schiff bases: Synthesis, spectroscopic characterization and catalytic activity in sulfoxidation and epoxidation. *InorganicaChimicaActa*, 511, 119832.
- [16]. Shetty, P. (2020). Schiff bases: An overview of their corrosion inhibition activity in acid media against mild steel. *Chemical Engineering Communications*, 207(7), 985-1029.
- [17]. Abdel-Rahman, L. H., Abu-Dief, A. M., Adam, M. S. S., &Hamdan, S. K. (2016). Some new nano-sized mononuclear Cu (II) Schiff base complexes: design, characterization, molecular modeling and catalytic potentials in benzyl alcohol oxidation. *Catalysis Letters*, 146(8), 1373-1396.
- [18]. Manimaran, A., Prabhakaran, R., Deepa, T., Natarajan, K., &Jayabalakrishnan, C. (2008). Synthesis, spectral characterization, electrochemistry and catalytic activities of Cu (II) complexes of bifunctional tridentate Schiff bases containing O \square N \square O donors. *Applied Organometallic Chemistry*, 22(7), 353-358.
- [19].Kocaokutgen, H., and Erdem, E., 2004. Synthesis and Spectral Characterization of Metal Complexes of 1-(2-Hydroxy-4-methylphenylazo)-2-naphthol. *Synthesis and Reactivity in Inorganic and Metal-Organic Chemistry*, 34(10), pp.1843-1853.
- [20]. Law, K. Y., Tarnawskyj, I. W., and Lubberts, P. T., 1993. Azo pigments and their intermediates: Effect of substitution on the diazotization and coupling reactions of o-hydroxyanilines. *Dyes and pigments*, 23(4), pp.243-254.
- [21]. Baron EJ, Finegold SM (1990) Diagnostic Microbiology. 8th Ed. Mosby Company. London., 53-62
- [22].SilverschtiénR.M., Bassler and Morril, “Spectrophotometers Identification of Organic Compound”, Translated by Ali Hussain and Suphi Al-Azawi. 1981.
- [23].Mohan, C., Kumar, V., Kumari, N., Kumari, S., Yadav, J., Gandass, T., and Yadav, S., 2020. Synthesis, Characterization and Antibacterial Activity of Semicarbazide Based Schiff Bases and their Pb (II), Zr (IV) and U (VI) Complexes. *J. Adv. Chem*, 2, pp.187-196.
- [24].Swati, G., Romila, K., Sharma, I. K., and Verma, P. S., 2011. Synthesis, characterization and antimicrobial screening of some azo compounds. *Int. J. Appl. Biol. Pharm. Tech*, 2(2), pp.332-38.
- [25].Hussein, S. A., and Yousif, E. I., 2021. New Mannich Base (2R)-4-methyl-2-((S)(phenylamino)(p-tolyl) methyl) cyclohexan-1-one; Synthesis and Spectral Characterisation. In *Journal of Physics: Conference Series* (Vol. 1999, No. 1), pp.012019.
- [26].Alasmi, A., and Merza, J., 2017. Synthesis and characterization of novel dialdehydes based on SN2 reaction of aromatic aldehyde. *Inorg. Chem. Ind. J*, 12(1), pp.111.
- [27].Baraa Kasim Mohammed and Enaam Ismail Yousif.,(Synthesis, Structural Characterisation and Biological Activity; New Metal Complexes Derived from Semicarbazone Ligand)., Revis Bionatur.,Volume 8 / Issue 2 / 14/2023
- [28]. Sharghi H, Jokar M (2009) Highly stereo selective facile synthesis of β -amino carbonyl compounds via a Mannich-type reaction catalyzed by γ -Al₂O₃/MeSO₃H (alumina/methanesulfonic acid: AMA) as a recyclable, efficient, and versatile heterogeneous catalyst, *Can. J. Chem.*, 88: 14-26.
- [29]. Hasan A. Hasan, Enaam I. Yousif, Mohamad J. Al-Jeboori.,Metal-assisted assembly of dinuclear metal(II) dithiocarbamate Schiff-base macrocyclic complexes: Synthesis and biological studies.,2012 *Global Journal of Inorganic Chemistry*.,1,2, 132-138
- [30].Lever ABP (1984) *Inorganic Electronic Spectroscopy*, 2nd Ed., New York,.
- [31]. Singh RV, Dwivedi R, Joshi SC (2004) Synthetic, magnetic, spectral, antimicrobial and antifertility studies of dioxomolybdenum(VI) unsymmetrical imine complexes having a N \cap N donor system, *Transition Met. Chem.*, 29(1): 70- 74.
- [32]. Ramesh R, Maheswaran S (2003) Synthesis, spectra, dioxygen affinity and antifungal activity of Ru(III) Schiff base complexes, *J. Inorg .Biochem.*, 96: 457-462.

- [33]. Rahman A, Choudhary M, Thomsen W (2001) Bioassay Techniques for Drug Development, Harwood Academic.
- [34].Enaam I. Y., New mixed ligand complexes; Synthesis, spectral analysis and biological activity(2019),Journal of Global Pharma Technology,11(2), pp. 196–203.
- [35].Hala Mohammed Salh and Taghreed H Al-Noor.,Preparation, Structural Characterization and Biological Activities of Curcumin-Metal(II)-L-3,4-dihydroxyphenylalanin(L-dopa)complexes, Ibn Al-Haitham Journal for Pure and Applied Sciences, 36(1)2023
- [36].Amer J. Jarad a, Marwa Ali Dahi a, Taghreed H. Al-Noor a, Marei M. El-ajaily b, Salam R. AL-Ayash a, AlyAbdou c, (Synthesis, spectral studies, DFT, biological evaluation, molecular docking and dyeing performance of 1-(4-((2-amino-5-methoxy)diazenyl)phenyl) ethanone complexes with some metallic ions) Journal of Molecular Structure, 1287 (2023) 135703
- [37]. Baidaa K Al-Rubaye, Nasry Jassim Hussien, Abdul Salam A Abul Rahman, Siti Fairus M Yusoff, Enaam I Yousif, Mohamad J Al-Jeboori.,NEW ORGANOTIN(IV) COMPLEXES DERIVED FROM 3,4- DIHYDROXYBENZALDEHYDEN(4)-ETHYL-3-SEMICARBAZONE LIGAND : SYNTHESIS, CHARACTERISATION AND BIOLOGICAL ACTIVITY., Biochem. Cell. Arch. Vol. 20, No. 2, pp. 6571-6579, 2020.
- [38]. Mohamad J. Al-Jeboori and Safaudeen A. Hussain,. New Metal Complexes Derived from Mannich-Base Ligand; Synthesis, Spectral Characterisation and Biological Activity., | Journal of Global Pharma Technology|2019| Vol. 11| Issue 02 (Supl.) |548-560.

Fig 2: ^1H -NMR spectrum in DMSO- d_6 solutions of HL.

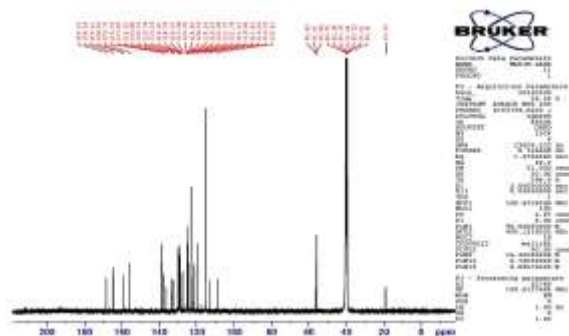


Fig 3: ^{13}C -NMR spectrum in DMSO- d_6 solutions of HL.

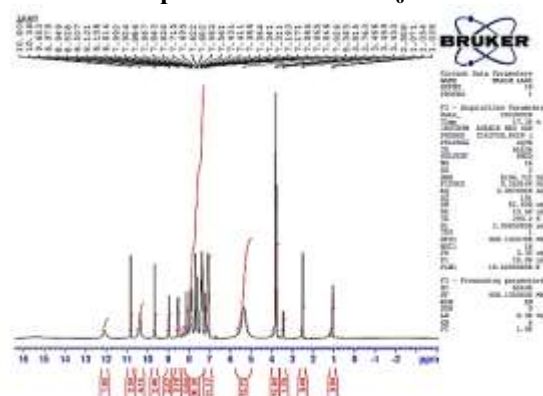


Fig 4: electrospray (+) mass spectrum of HL.

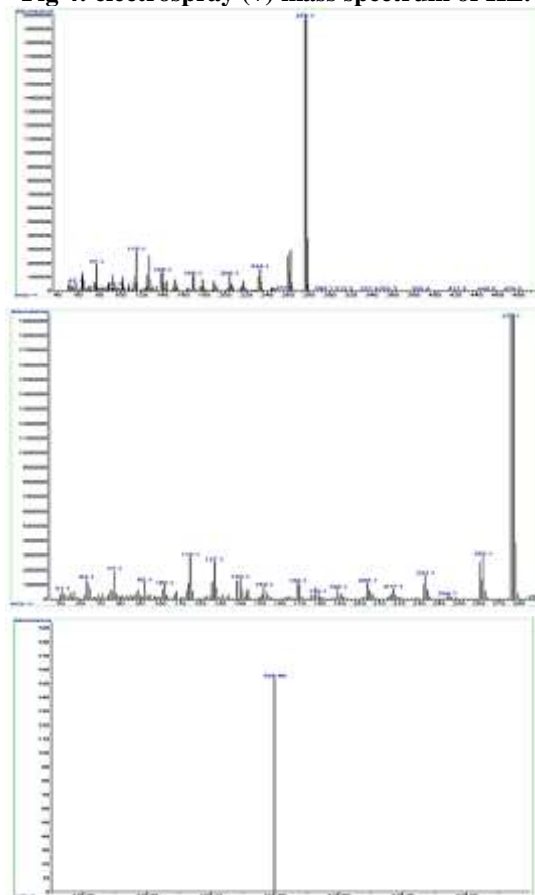


Fig 5. The TGA thermal curve of HL in an atmosphere of Ar.

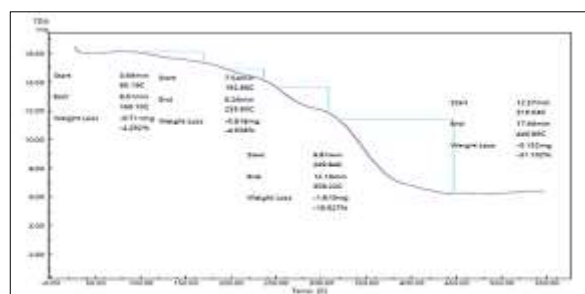
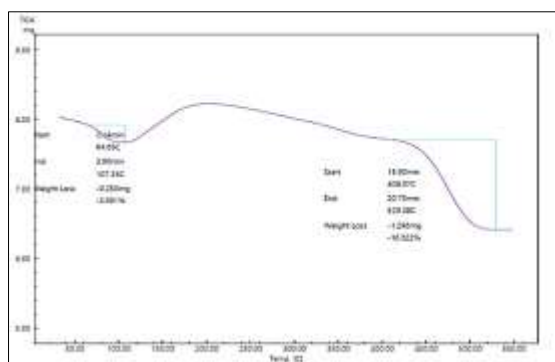


Fig 6. Thermal decomposition of [Co(L)Cl].H₂O in an atmosphere of Ar.

معقدات معدنية جديدة مشتقة من ليكاندقاعدة شيف المرتبطة بالآزو: التحضير والتشخيص

الطيفي والتقييم البيولوجي

مريم باسم حمزة ، انعام اسماعيل يوسف

قسم الكيمياء، كلية التربية للعلوم الصرفة ابن الهيثم، جامعة بغداد

anaam.i.y@ihcoedu.uobaghdad.edu.iq

الخلاصة

ومعدنات المعنيدية الاحادية p-anisidine تم تحضير وتشخيص ليكاند أزو- قاعدة شف الجديدة ومشتقمنليكاند هو :

(1-((E)-((4-methoxy phenyl) imino) methyl)-3-((E)-(4-nitrophenyl)diazenyl) naphthalen-2-ol) (HL),

حصلنا عليه من خلال مفاعلة:

1:1 بنسب مولية p-anisidine و (E)-2-hydroxy-3-((4-nitrophenyl)diazenyl)-1-naphthaldehyde) مع بعض العناصر المعدنية المختارة HL تفاعلا لنتيجة تكون معقدات احادية التناسق (L:M), 1:1 بنسب مولية Cu^{II} و Cr^{III} , Mn^{II} , Co^{II} , Ni^{II} وهي شخّصت الليكاندات والمعدّات بواسطة التحليل الدقيق للعناصر، محتوى المعدن والكُلور، مطياف الاشعة تحت الحمراء، ومطياف الاشعة فوق البنفسجية والرنين النووي المغناطيسي ومطيافية الكتلة بالإضافة الى فحص الحساسية المغناطيسية، التوصيلية المولارية و درجات الانصهار أكدت بيانات التشخيص تكوين مركبات سداسية التناسق واخرى رباعية التناسق Co ولمعقد HL الليكاند (TGA) تم فحص الاستقرار الحراريتم استكشاف النشاط المضاد للميكروبات للمركبات المحضرة تجاه العديد من الكائنات الحية الدقيقة البكتيريا (والفطريات) وتظهر البيانات التي تم جمعها أن النشاط المضاد للميكروبات لليكاند قد تحسن بعد تكوين معقدات.